

# Topological Aspects of Charge-Carrier Transmission across Grain Boundaries in Graphene

Fernando Gargiulo and Oleg V. Yazyev

*Institute of Theoretical Physics, Ecole Polytechnique Fédérale de Lausanne (EPFL), CH-1015 Lausanne, Switzerland*

(Dated: June 28, 2021)

We systematically investigate the transmission of charge carriers across the grain-boundary defects in polycrystalline graphene by means of the Landauer-Büttiker formalism within the tight-binding approximation. Calculations reveal a strong suppression of transmission at low energies upon decreasing the density of dislocations with the smallest Burger's vector  $\mathbf{b} = (1, 0)$ . The observed transport anomaly is explained from the point of view of back-scattering due to localized states of topological origin. These states are related to the gauge field associated with all dislocations characterized by  $\mathbf{b} = (n, m)$  with  $n - m \neq 3q$  ( $q \in \mathbb{Z}$ ). Our work identifies an important source of charge-carrier scattering caused by topological defects present in large-area graphene samples produced by chemical vapor deposition.

PACS numbers: 73.22.Pr, 72.80.Vp, 61.72.Lk, 61.72.Mm

Since its isolation in 2004 [1], graphene has been attracting ever-increasing attention due to its extraordinary physical properties and potential technological applications [2–4]. Early research experiments on graphene have been performed using single micrometer-scale samples obtained by micromechanical cleavage. However, technological applications require manufacturing processes that would allow for robust production at much larger scales, e.g. chemical vapor deposition technique [5–7]. Recent experimental studies have shown that such extended graphene samples tend to be polycrystalline, i.e. composed of micrometer-size single-crystalline domains of varying lattice orientation [8–10]. Dislocations and grain boundaries are responsible for breaking the long-range order in polycrystals. These topological defects inevitably affect all physical properties of graphene [11–17]. In particular, it has been demonstrated experimentally that grain boundaries dramatically alter the electronic transport properties of graphene [18–20]. Understanding the effect of topological defects on charge-carrier transport in graphene is crucial for technological applications of this material in electronics, clean energy and related domains.

According to the Read-Shockley model [21], grain boundaries in two-dimensional crystals are equivalent to one-dimensional arrays of dislocations. In graphene, the low-energy configurations of the cores of constituent dislocations are composed of pairs of pentagons and heptagons, with the resulting Burger's vector dependent on their mutual positions [22–25]. Remarkably, in certain highly ordered grain-boundary structures the conservation of momentum results in a complete suppression of the transmission of low-energy charge carriers [11]. However, it is of paramount importance to understand the factors determining the charge-carrier transmission probability in a more general situation when no symmetry-related selection is present. For example, this is the case of grain boundaries with strongly perturbed periodic ar-

range of dislocations, such as the ones observed in graphene grown by chemical vapor deposition [8, 9].

In this Letter, we report a systematic study of the charge-carrier transmission across grain boundaries in graphene by means of the Landauer-Büttiker approach. We find that the structural topological invariant of dislocations [26], the Burger's vector  $\mathbf{b}$ , plays a crucial role in determining transport properties. In particular, for the case of grain boundaries formed by the minimal Burger's vector  $\mathbf{b} = (1, 0)$  dislocations, we find an unexpected suppression of the transmission of low-energy charge carriers in the limit of small misorientation angles (or, equivalently, small dislocation densities). This counter-intuitive behavior is explained from the point of view of resonant back-scattering involving localized states of topological origin, which arise due to the gauge field created by dislocations characterized by  $\mathbf{b} = (n, m)$  with  $n - m \neq 3q$  ( $q \in \mathbb{Z}$ ). The  $\mathbf{b} = (1, 1)$  dislocations are shown to behave as ordinary scattering centers and have very weak effects on the electronic transport.

In our study we employ the nearest-neighbor tight-binding model Hamiltonian

$$H = -t \sum_{\langle i, j \rangle} [c_i^\dagger c_j + \text{h.c.}], \quad (1)$$

where  $c_i$  ( $c_i^\dagger$ ) annihilates (creates) an electron at site  $i$  and  $\langle i, j \rangle$  stands for pairs of nearest-neighbor atoms. The hopping integral  $t = 2.7$  eV is assumed to be constant [27]. Coherent transport across grain boundaries in graphene is studied within the Landauer-Büttiker formalism which relates the conductance  $G(E)$  at a given energy  $E$  to the transmission  $T(E)$  as  $G(E) = G_0 T(E)$ , with  $G_0 = 2e^2/h$  being the conductance quantum [28]. The transmission is evaluated by means of the non-equilibrium Green's function approach using two-terminal device configurations, with contacts represented by the semi-infinite ideal graphene leads:

$$T = \text{Tr}[\Gamma_L G_S^\dagger \Gamma_R G_S]. \quad (2)$$

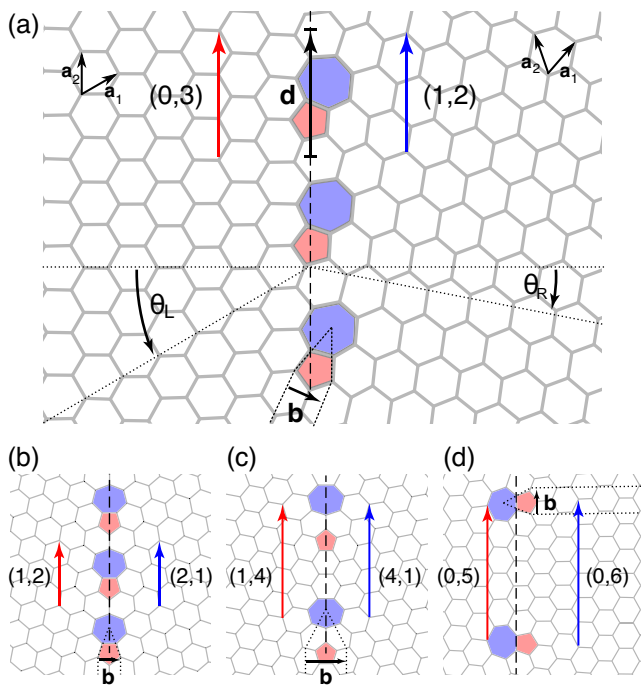


FIG. 1: (Color online) (a) A generic example of asymmetric periodic grain boundary composed of  $\mathbf{b} = (1, 0)$  dislocations. This grain-boundary structure is characterized by rotation angles  $\theta_L = 30^\circ$  and  $\theta_R = 10.9^\circ$ , and a pair of matching vectors  $(0, 3)|(1, 2)$ . The periodicity vector  $\mathbf{d}$  and the Burger's vector  $\mathbf{b}$  are shown. Structures of symmetric grain boundaries formed by (b)  $\mathbf{b} = (1, 0)$  and (c)  $\mathbf{b} = (1, 1)$  dislocations. (d) Degenerate grain boundary ( $\theta = 0^\circ$ ) with the Burger's vector of constituent dislocations oriented along the grain-boundary line (shown as dashed line).

The scattering region Green's function  $G_S$  is calculated as

$$G_S = [E^+ I - H_S - \Sigma_L - \Sigma_R]^{-1} \quad (3)$$

employing the coupling matrices  $\Gamma_{L(R)}$  for the left (right) lead given by

$$\Gamma_{L(R)} = i[\Sigma_{L(R)} - \Sigma_{L(R)}^\dagger]. \quad (4)$$

In these expressions  $H_S$  is the Hamiltonian for the scattering region,  $\Sigma_{L(R)}$  are the self-energies which couple scattering region to the leads and  $E^+ = E + i\eta I$  ( $\eta \rightarrow 0^+$ ). The dependence of  $T$ ,  $G_S$ ,  $\Gamma_{L(R)}$  and  $\Sigma_{L(R)}$  on energy  $E$  and transverse momentum  $k_{\parallel}$  is omitted for the sake of compact notation.

We consider grain-boundary models constructed as periodic arrays of dislocations following the Read-Shockley model [21]. Only dislocations formed by pentagons and heptagons are investigated as these structures preserve the three-fold coordination of  $sp^2$  carbon atoms thus ensuring energetically favorable configurations of defects. This construction is consistent with experimental atomic resolution images of grain boundaries in polycrystalline

graphene [8, 9]. The relative positions of pentagons and heptagons defines the Burger's vectors of constituent dislocations. The Burger's vectors, their orientation with respect to the grain boundary line, and the distance between dislocation cores define the grain boundary's structural topological invariant—the misorientation angle  $\theta = \theta_L + \theta_R$ . This relation allows constructing arbitrary grain boundary models, as described in Ref. 22. Alternatively, periodic grain boundaries can be defined in terms of a pair of matching vectors  $(n_L, m_L)|(n_R, m_R)$ , introduced in Ref. 11 [Fig. 1(a)]. In this paper, however, we shall constrain our discussion to the Burger's vectors  $\mathbf{b}$  and the inter-dislocation distances  $d$  in order to simplify the discussion. Figure 1(a) shows a generic example of an asymmetric grain boundary formed by the  $\mathbf{b} = (1, 0)$  dislocations. Figures 1(b) and 1(c) depict examples of symmetric ( $\theta_L = \theta_R$ ) periodic grain boundaries formed by  $\mathbf{b} = (1, 0)$  and  $\mathbf{b} = (1, 1)$  dislocations, respectively. Figure 1(d) shows an example of a degenerate grain boundary ( $\theta = 0^\circ$ ) with the Burger's vector of constituent dislocations oriented along the grain boundary line. In our study, we focus only on the models that do not result in transport gaps due to selection by momentum [29].

We first focus on symmetric periodic grain boundaries formed by  $\mathbf{b} = (1, 0)$  ( $=2.46 \text{ \AA}$ ) dislocations. Such grain boundaries are defined by pairs of matching vectors belonging to the  $(l, l+1)|(l+1, l)$  series ( $l \in \mathbb{N}$ ). Hence,  $d = a_0 \sqrt{3l(l+1) + 1}$  where  $a_0 = 2.46 \text{ \AA}$  is the lattice constant of graphene. Figure 2(a) shows the transmission probability  $T$  as a function of energy  $E$  and transverse momentum  $k_{\parallel}$  for the first member of this sequence ( $l = 1$ ) characterized by  $d = 6.51 \text{ \AA}$  [Fig. 1(b)]. One clearly observes a projected Dirac cone in the irreducible half of the one-dimensional Brillouin zone corresponding to the periodic grain-boundary structure with  $T(k_{\parallel}, E) \lesssim 1$ , in agreement with previous calculations [11]. Figure 2(b) shows  $T(k_{\parallel}, E)$  for a grain boundary characterized by  $l = 8$  and, hence, a larger periodicity  $d = 36.2 \text{ \AA}$ . The most evident difference between the two is the occurrence of multiple conductance channels as a result of band folding over smaller Brillouin zone. The striking feature, however, is the clear reduction of conductance close to the Dirac point energy  $E = 0$ . The counter-intuitive decrease of transmission or, equivalently, enhancement of scattering upon decreasing the density of dislocations suggests the topological origin of the observed transport behavior. Figures 2(c) and 2(d) further investigate the details of charge-carrier transmission at very low energy ( $E = 10^{-3}t$ ). One clearly observes a monotonic decrease of  $T(q_{\parallel})$  (with  $q_{\parallel} = k_{\parallel} - (2\pi)/(3d)$  being the transverse momentum relative to the location of the projected Dirac point) as  $d$  increases [Fig. 2(c)]. The transmission probability of normally incident charge carriers ( $q_{\parallel} = 0$ ) exhibits an inverse power scaling law  $T \propto d^{-\gamma}$ , with an

exponent  $\gamma \approx 0.5$  [dashed lines in Fig. 2(d)]. Moreover, the observed scaling law is independent of the orientation of the Burger's vectors of dislocations relative to the grain-boundary line. This was explicitly demonstrated using several models of asymmetric and degenerate grain boundaries [Fig. 2(d)].

The observed transport anomaly is further investigated by analyzing the local density of states (LDOS) calculated as

$$\text{LDOS}_n(E) = -\frac{d}{\pi^2} \int_0^{\pi/d} \text{Im}(G_S(E, k_{\parallel}))_{n,n} dk_{\parallel}. \quad (5)$$

Figure 3(a) shows the density of states (DOS) calculated by summing the LDOS over atoms located in the grain-boundary region of 40 Å width. One clearly observes the presence of sharp van Hove singularities both in the valence and conduction bands superimposed on the linear contribution of pristine graphene. The peak positions converge to the Dirac point energy as the distance between dislocations  $d$  increases [Fig. 3(b)]. These DOS peaks can be attributed to the electronic states localized at the dislocations, as corroborated by Figure 3(c).

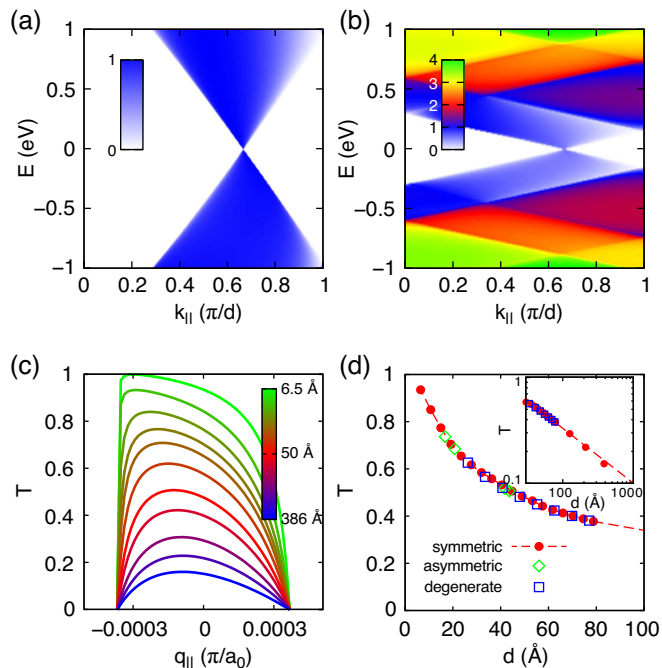


FIG. 2: (Color online) Electronic transport across periodic grain boundaries in graphene formed by the  $\mathbf{b} = (1, 0)$  dislocations. (a),(b) Transmission probability as a function of energy  $E$  and transverse momentum  $k_{\parallel}$  across symmetric grain boundaries characterized by  $d = 6.51$  Å and  $d = 36.2$  Å, respectively. (c) Transmission probability close to the Dirac point ( $E = 10^{-3}t$ ) as a function of  $q_{\parallel}$  for different values of  $d$ . (d) Low-energy transmission of the normally-incident charge carriers as a function of inter-dislocation distance  $d$  for symmetric, asymmetric and degenerate grain boundaries. The inset shows the logarithmic scale plot.

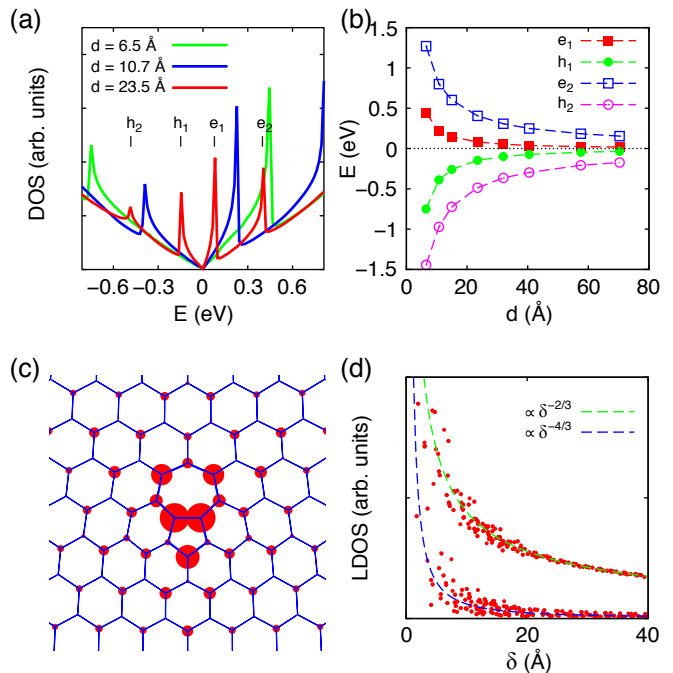


FIG. 3: (Color online) (a) Density of states (DOS) in the interface region computed for the grain boundaries formed by  $\mathbf{b} = (1, 0)$  dislocations with different values of  $d$ . (b) Positions of the DOS peaks as a function of  $d$ . The labels refer to peaks in panel (a) shown for the  $d = 23.5$  Å grain boundary. (c) Local density of states (LDOS) at  $E = 10^{-3}t$  for the  $d = 61.8$  Å grain boundary. Circle areas are proportional to the LDOS. (d) LDOS as a function of distance from the defect core  $\delta$  calculated at  $E = 10^{-3}t$  for the  $d = 385$  Å grain boundary. Solid lines indicate two trends consistent with the results of Ref. 41.

The presence of localized states results in resonant back-scattering at low energies, similar to dopants and covalent functionalization defects in graphene [30–35].

The origin of the localized states is related to the topological nature of defects in polycrystalline graphene. Charge carriers of momentum  $\mathbf{k}$  encircling a dislocation with Burger's vector  $\mathbf{b}$  gain a phase  $\varphi = \mathbf{k} \cdot \mathbf{b}$  [36]. The aforementioned  $\mathbf{b} = (1, 0)$  dislocations thus give rise to  $\varphi = +2\pi/3$  and  $\varphi = -2\pi/3$  for the charge carriers in valleys  $\tau = +1$  and  $\tau = -1$ , respectively. Starting from the Dirac equation for a massless particle

$$H = (p_x - iA_x) \sigma_x + (p_y - iA_y) \tau \sigma_y, \quad (6)$$

the effect of a dislocation is accounted for by means of a gauge field  $\mathbf{A} \propto \mathbf{k} \cdot \mathbf{b}$  [37–40]. Using this continuum model, Mesáros *et al.* predicted that an isolated  $\mathbf{b} = (1, 0)$  dislocation gives rise to quasi-localized modes at  $E = 0$  [41]. The continuous model for  $\mathbf{b} = (1, 0)$  has two low-energy solutions with the LDOS decaying as  $\propto \delta^{-2/3}$  and  $\propto \delta^{-4/3}$ , where  $\delta$  is the distance from the defect core. Our numerical calculations for the grain-boundary model with a very large distance between dislocations confirm

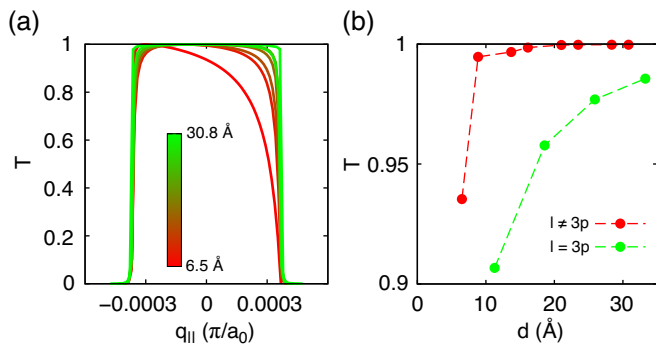


FIG. 4: (Color online) Electronic transport across grain boundaries composed of  $\mathbf{b} = (1, 1)$  dislocations. (a) Transmission probability close to the Dirac point ( $E = 10^{-3}t$ ) as a function of  $q_{||}$  for grain boundaries characterized by different values of  $d$  within the  $l \neq 3p$  family. (b) Low-energy transmission of the normally-incident charge carriers as a function of inter-dislocation distance  $d$ . Two families of grain boundaries are distinguished.

the analytical result showing the two solutions coexisting on different sublattices of the graphene lattice [Fig. 3(d)].

In order to gain a qualitative understanding of the dependence of transmission on  $d$  [Figs. 2(c) and 2(d)], one has to appreciate the fact that the finite distance between dislocations forming a grain boundary allows for the hybridization of localized states. As a result, the LDOS peaks at positive and negative energies emerge in lieu of the  $E = 0$  peak for an isolated dislocation. As the distance between dislocations  $d$  increases, the hybridization diminishes, thus reducing the peak energies [Figs. 3(a) and 3(b)] and resulting in the progressive decrease of the transmission close to  $E = 0$ . At finite energies, however, the minimum of transmission is achieved at a certain distance between dislocations. It is worth stressing that despite the fact that our conclusions are based on periodic models of dislocations, there is no strict requirement of periodicity, in contrast to the case of suppressed conductivity due to momentum conservation [11]. This has been explicitly verified by means of supercell calculations which show that transmission is insensitive to perturbation of the periodic arrangement of dislocations in grain boundaries.

More generally, all dislocations characterized by Burger's vectors  $\mathbf{b} = (n, m)$  with  $n - m \neq 3q$  ( $q \in \mathbb{Z}$ ) have a similar effect on charge carriers in graphene because of equal values for the  $\mathbf{k} \cdot \mathbf{b}$  product for the two valleys. However, dislocations with  $n - m = 3q$  are expected to behave as ordinary (topologically trivial) scatterers since  $\mathbf{k} \cdot \mathbf{b} = 0$ . We verify this statement by investigating the transmission through the grain boundaries formed by  $\mathbf{b} = (1, 1)$  ( $= 4.23$  Å) dislocations [Fig. 1(c)]. Following the convention defined earlier, these grain boundaries are defined by the pairs of matching vectors belonging to  $(1, l + 1)|(l + 1, 1)$  series ( $l \in \mathbb{N}$ ). Figure 4(a) shows that

already the first members of this family exhibit transmission probabilities close to 1, which further increase as the inter-dislocation distance  $d$  increases. Moreover, one can distinguish two families of grain-boundary structures characterized by  $l = 3p$  and  $l \neq 3p$  ( $p \in \mathbb{N}$ ) [Fig. 4(b)]. Within both families the effect of dislocations can be described in terms of scattering cross-sections,  $\sigma_{l=3p} \approx 0.5$  Å and  $\sigma_{l \neq 3p} \approx 0.01$  Å. The first value is significantly larger since both Dirac points correspond to  $k_{||} = 0$ , thus enabling the intervalley scattering process upon transmission. The LDOS calculated for these grain boundary configurations show no localized states at low energies (not shown here).

To conclude, our study reveals an intriguing aspect of charge-carrier transport in topologically disordered graphene. Predicted anomalous scattering is especially pertinent to low-angle grain boundaries ( $d \gg |\mathbf{b}|$ ) composed of dislocations with the minimal Burger's vector  $\mathbf{b} = (1, 0)$ . These dislocations are dominant in realistic samples due to the reduced elastic response [26], and may even occur within seemingly single-crystalline domains of graphene [42]. Unlike covalently bound adatoms which also act as resonant scattering centers [31–35], dislocations cannot be easily eliminated from the sample due to their topological nature and high diffusion barriers at normal conditions [43]. Our work thus identifies an important source of charge-carrier scattering in large-area samples of graphene produced by high efficiency techniques, such as the chemical vapor deposition.

We would like to thank G. Autès, A. Cortijo, M. I. Katsnelson, L. S. Levitov, and A. Mesaros for discussions. This work was supported by the Swiss National Science Foundation (Grant No. PP00P2\_133552). Computations have been performed at the Swiss National Supercomputing Centre (CSCS) under project s443.

- 
- [1] K. S. Novoselov, A. K. Geim, S. V. Morozov, D. Jiang, Y. Zhang, S. V. Dubonos, I. V. Grigorieva and A. A. Firsov, *Science* **306**, 666 (2004).
  - [2] A. K. Geim and K. S. Novoselov, *Nature Mater.* **6**, 183 (2007).
  - [3] M. I. Katsnelson, *Materials Today* **10**, 20 (2007).
  - [4] A. H. Castro Neto, F. Guinea, N. M. R. Peres, K. S. Novoselov, and A. K. Geim, *Rev. Mod. Phys.* **81**, 109 (2009).
  - [5] K. S. Kim, Y. Zhao, H. Jang, S. Y. Lee, J. M. Kim, K. S. Kim, J.-H. Ahn, P. Kim, J.-Y. Choi, and B. H. Hong, *Nature (London)* **457**, 706 (2009).
  - [6] X. Li, W. Cai, J. An, S. Kim, J. Nah, D. Yang, R. Piner, A. Velamakanni, I. Jung, E. Tutuc, S. K. Banerjee, L. Colombo, and R. S. Ruoff, *Science* **324**, 1312 (2009).
  - [7] S. Bae, H. Kim, Y. Lee, X. Xu, J.-S. Park, Y. Zheng, J. Balakrishnan, T. Lei, H. Ri Kim, Y. I. Song, Y.-J. Kim, K. S. Kim, B. Özyilmaz, J.-H. Ahn, B. H. Hong, and S. Iijima, *Nature Nanotechnol.* **5**, 574 (2010).

- [8] P. Y. Huang, C. S. Ruiz-Vargas, A. M. van der Zande, W. S. Whitney, M. P. Levendorf, J. W. Kevek, S. Garg, J. S. Alden, C. J. Hustedt, Y. Zhu, J. Park, P. L. McEuen, and D. A. Muller, *Nature (London)* **469**, 389 (2011).
- [9] K. Kim, Z. Lee, W. Regan, C. Kisielowski, M. F. Crommie, and A. Zettl, *ACS Nano* **5**, 2142 (2011).
- [10] J. An, E. Voelkl, J. W. Suk, X. Li, C. W. Magnuson, L. Fu, P. Tiemeijer, M. Bischoff, B. Freitag, E. Popova, and R. S. Ruoff, *ACS Nano* **5**, 2433 (2011).
- [11] O. V. Yazyev and S. G. Louie, *Nature Mater.* **9**, 806 (2010).
- [12] R. Grantab, V. B. Shenoy, and R. S. Ruoff, *Science* **330**, 946 (2010).
- [13] D. Gunlycke and C. T. White, *Phys. Rev. Lett.* **106**, 136806 (2011).
- [14] A. Ferreira, X. Xu, C.-L. Tan, S.-K. Bae, N. M. R. Peres, B.-H. Hong, B. Özyilmaz, and A. H. Castro Neto, *Europhys. Lett.* **94**, 28003 (2011).
- [15] Y. Wei, J. Wu, H. Yin, X. Shi, R. Yang, and M. Dresselhaus, *Nature Mater.* **11**, 759 (2012).
- [16] D. Van Tuan, J. Kotakoski, T. Louvet, F. Ortman, J. C. Meyer, and S. Roche, *Nano Lett.* **13**, 1730 (2013).
- [17] T. M. Radchenko, A. A. Shylau, I. V. Zozoulenko and A. Ferreira, *Phys. Rev. B* **87**, 195448 (2013).
- [18] Q. Yu, L. A. Jauregui, W. Wu, R. Colby, J. Tian, Z. Su, H. Cao, Z. Liu, D. Pandey, D. Wei, T. F. Chung, P. Peng, N. P. Guisinger, E. A. Stach, J. Bao, S.-S. Pei, and Y. P. Chen, *Nature Mater.* **10**, 443 (2011).
- [19] A. W. Tsien, L. Brown, M. P. Levendorf, F. Ghahari, P. Y. Huang, R. W. Havener, C. S. Ruiz-Vargas, D. A. Muller, P. Kim, and J. Park, *Science* **336**, 1143 (2012).
- [20] J. C. Koepke, J. D. Wood, D. Estrada, Z.-Y. Ong, K. T. He, E. Pop, and J. W. Lyding, *ACS Nano* **7**, 75 (2012).
- [21] W. T. Read and W. Shockley, *Phys. Rev.* **78**, 275 (1950).
- [22] O. V. Yazyev and S. G. Louie, *Phys. Rev. B* **81**, 195420 (2010).
- [23] Y. Liu and B. I. Yakobson, *Nano Lett.* **10**, 2178 (2010).
- [24] A. Carpio, L. L. Bonilla, F. de Juan, and M. A. H. Vozmediano, *New J. Phys.* **10**, 053021 (2008).
- [25] J. M. Carlsson, L. M. Ghiringhelli, and A. Fasolino, *Phys. Rev. B* **84**, 165423 (2011).
- [26] D. R. Nelson, *Defects and geometry in condensed matter physics*. (Cambridge University Press, Cambridge, 2002).
- [27] We verified by means of explicit calculations that including the dependence of hopping integrals on the variations of interatomic distance due to the elastic strain fields produced by the dislocations has only minor effect on the low-energy charge-carrier transmission. The tight-binding results also agree with the results of first-principles calculations as shown previously [11].
- [28] M. Büttiker, Y. Imry, R. Landauer, and S. Pinhas, *Phys. Rev. B* **31**, 6207 (1985).
- [29] Only periodic structures characterized by marching vectors  $(n_L, m_L)|(n_R, m_R)$  such that either both  $n_L - m_L = 3p$  and  $n_R - m_R = 3q$ , or both  $n_L - m_L \neq 3p$  and  $n_R - m_R \neq 3q$  ( $p, q \in \mathbb{Z}$ ) are considered [11].
- [30] H. J. Choi, J. Ihm, S. G. Louie, and M. L. Cohen, *Phys. Rev. Lett.* **84**, 2917 (2000).
- [31] M. Titov, P. M. Ostrovsky, I. V. Gornyi, A. Schuessler, and A. D. Mirlin, *Phys. Rev. Lett.* **104**, 076802 (2010).
- [32] T. O. Wehling, S. Yuan, A. I. Lichtenstein, A. K. Geim, and M. I. Katsnelson, *Phys. Rev. Lett.* **105**, 056802 (2010).
- [33] S. Yuan, H. De Raedt, and M. I. Katsnelson, *Phys. Rev. B* **82**, 115448 (2010).
- [34] A. Ferreira, J. Viana-Gomes, J. Nilsson, E. R. Mucciolo, N. M. R. Peres, and A. H. Castro Neto, *Phys. Rev. B* **83**, 165402 (2011).
- [35] T. M. Radchenko, A. A. Shylau, and I. V. Zozoulenko, *Phys. Rev. B* **86**, 035418 (2012).
- [36] S. V. Iordanskii and A. E. Koshelev, *Sov. Phys. JETP* **63**, 820 (1986); *ibid.* **64**, 190 (1986).
- [37] P. E. Lammert and V. H. Crespi, *Phys. Rev. Lett.* **85**, 5190 (2000).
- [38] A. Cortijo and M. A. H. Vozmediano, *Nucl. Phys. B* **763**, 293 (2007).
- [39] A. Mesaros, D. Sadri, and J. Zaanen, *Phys. Rev. B* **79**, 155111 (2009).
- [40] M. A. H. Vozmediano, M. I. Katsnelson, and F. Guinea, *Phys. Rep.* **496**, 109 (2010).
- [41] A. Mesaros, S. Papanikolaou, C. F. J. Flipse, D. Sadri, and J. Zaanen, *Phys. Rev. B* **82**, 205119 (2010).
- [42] J. Coraux, A. T. N'Diaye, C. Busse, and T. Michely, *Nano Lett.* **8**, 565 (2008).
- [43] F. Banhart, J. Kotakoski, and A. V. Krasheninnikov, *ACS Nano* **5**, 26 (2010).